NEOPLASIA
www.neoplasia.com

Volume 25 Number C March 2022 pp. 1–8

Towards a molecular understanding of the overlapping and distinct roles of UBQLN1 and UBQLN2 in lung cancer progression and metastasis

Parag P. Shah [a]; Kumar Saurabh [a]; Zimple Kurlawala [a]; Alexis A. Vega [b]; Leah J. Siskind [a,d]; Levi J. Beverly [a,b,c,d,*]

[a] James Graham Brown Cancer Center, University of Louisville, 505 S. Hancock Street, CTRB rm 204, Louisville, KY 40202, USA
[b] Department of Biochemistry and Molecular Genetics, University of Louisville, Louisville, KY 40202, USA
[c] Department of Medicine, Division of Hematology and Oncology, University of Louisville School of Medicine, Louisville, KY 40202, USA
[d] Department of Pharmacology and Toxicology, University of Louisville School of Medicine, Louisville, KY 40202, USA

Abstract

The Ubiquilin family of proteins (UBQLN) consists of five related proteins (UBQLN1-4 and UBQLNL) that all contain ubiquitin-like (UBL) and ubiquitin-associated (UBA) domains. UBQLN1 and UBQLN2 are the most closely related and have been the most well-studied, however their biochemical, biological and cellular functions are still not well understood. Previous studies from our lab reported that loss of UBQLN1 or UBQLN2 induces epithelial mesenchymal transition (EMT) in lung adenocarcinoma cells. Herein, we showed that loss of UBQLN1 and/or UBQLN2 induces cellular processes involved in tumor progression and metastasis, including proliferation, clonogenic potential and migration in lung adenocarcinoma cells. In fact, following simultaneous loss of both UBQLN1 and UBQLN2 many of these processes were further enhanced. To understand the molecular mechanisms by which UBQLN1 and UBQLN2 loss could be additive, we performed molecular, biochemical and RNAseq analyses in multiple cellular systems. We identified overlapping and distinct gene sets and pathways that were altered following loss of UBQLN1 and/or UBQLN2. We have also begun to define cell type specific gene regulation of UBQLN1 and UBQLN2, as well as understand how loss of either gene can alter differentiation of normal cells. The data presented here demonstrate that UBQLN1 and UBQLN2 perform similar, but distinct molecular functions in a variety of cell types.

Neoplasia (2022) 25, 1–8

Keywords: UBQLN1, UBQLN2, ERAD, RNAseq, EMT, Metastasis

Introduction

Ubiquilin1 (UBQLN1) and Ubiquilin2 (UBQLN2) belong to a family of proteins that have been suggested to be involved in various proteostatic processes, including endoplasmic reticulum-associated protein degradation (ERAD). It has been reported that UBQLN1 and UBQLN2 have been associated with various neurological disorders [1–3] however their biochemical, biological and cellular functions remain largely unknown, especially across various cell types including lung cancer cells. Previous work from our lab reported that, apart from their role in ERAD, they play an important role in induction of epithelial mesenchymal transition (EMT) in lung adenocarcinoma cells. Moreover, we showed that UBQLN1 is frequently lost and under expressed in lung cancer cell lines as well as human lung adenocarcinomas [4]. These observations have recently been confirmed by Zhang and Colleagues in A549 lung cancer cells [5]. Besides these findings, the role of UBQLN1 and UBQLN2 in regulating different cellular processes have been poorly understood.

In the present study, we provided evidence that loss of UBQLN1 and UBQLN2 induce EMT, increase cell proliferation, clonogenic potential and cell migration in lung adenocarcinoma cells. Interestingly, we observed further increase in many cellular processes following combined loss of both UBQLN1 and UBQLN2. Further, by performing immunoprecipitation experiment, we confirm work from others that UBQLN1 and UBQLN2 interact in cells. These data suggest a potential role for the hetero-multimers in cellular functions.

* Corresponding author at: James Graham Brown Cancer Center, University of Louisville, 505 S. Hancock Street, CTRB rm 204, Louisville, KY 40202, USA.
E-mail address: Levi.Beverly@Louisville.edu (L.J. Beverly).

Received 2 September 2021; received in revised form 29 October 2021; accepted 17 November 2021

https://doi.org/10.1016/j.neo.2021.11.010

With an effort to understand different cellular processes altered by UBQLN1 and UBQLN2 in different cell types, we performed bulk RNAseq analysis following siRNA-mediated loss of UBQLN1 and UBQLN2 in A549 (lung cancer) and SK-N-BE(2) (neuroblastoma), human induced pluripotent stem cells (iPSCs) and mouse embryonic stem cells (mESCs). In addition, we performed single cell RNAseq (scRNAseq) following differentiation of mES cells into either neuronal cells or epithelial cells with or without knockdown of UBQLN1. We identified unique genes that were significantly altered following loss of UBQLN1 in iPSCs and iPSCs differentiated either neuronal (iPSC-neuro) or epithelial (iPSC-epi) cells. Interestingly, t-Distributed Stochastic Neighbor Embedding (t-SNE) analysis revealed that knockdown of UBQLN1 drastically changed the identity of cells differentiated down the epithelial lineage, but neuronal differentiation was less altered.

Our data clearly demonstrate that both UBQLN1 and UBQLN2 have overlapping and distinct cellular functions including cell proliferation, clonogenic potential and cell migration and perform similar and distinct molecular functions in a variety of cell types.

Materials and methods

siRNA sequences used for study

All siRNAs used for study were ordered from Thermo Fisher Scientific Biosciences Inc. Lafayette, CO 80026, USA.

Non targeting siRNA (si_NT): UAAGGCUAUGAAGAGAUACAA
Kif11 siRNA (si_Kif11): Cat. No. AM4639
UBQLN1 siRNA (si_U1): GAAGAAAUCUCUAAACGUUUUUU
(si_U1-2): GUACUACUGCGCCAAAUUU
UBQLN2 siRNA (si_U2-5): CCUGGUAUCUCUAAGUAUAUU
(si_U2-6): GUAGAAUCUGAGUGUAAUAUU

Antibodies used for study

UBQLN1 #14526, UBQLN2 #85509, E-cadherin #3195, Vimentin # 5741, ZEB1 #3396, Snail #3879, Integrin $\beta 3$ #4702, p-Akt #9271, Akt #9272, GAPDH #2118, (Cell Signaling Technologies Inc. Danvers, MA 01923); Flag #F1804, (Sigma); pan-Ubqln polyclonal was made by inoculating rabbits with a peptide specific to the c-terminus of Ubqln1 (Yenzym Antibodies LLC).

Cell culture, siRNA transfection and protein analysis

Human lung adenocarcinoma cell line A549, neuroblastoma cell line SK-N-BE(2) and IMR90 fetal lung fibroblasts were purchased from American Type Culture Collection (ATCC, Rockville, MD, USA) and cultured in RPMI medium supplemented with 10% fetal bovine serum (Invitrogen, Carlsbad, CA, USA) and 1% antibiotic/antimycotic (Sigma, St Louis, MO, USA). The cell lines were routinely tested for mycoplasma and subcultured every 3–4 days. All siRNA transfections were performed using Dharmafect1 #T-2001-03 (Thermo Fisher Scientific Inc, Pittsburgh, PA, USA) as per manufacturer's protocol. After total 72 hrs of transfection cells were harvested in CHAPS lysis buffer (1% CHAPS detergent, 150mM NaCl, 50mM Tris pH 7, 5mM EDTA). Protein was quantitated by using Pierce's BCA Protein Assay Reagent Kit (# 23227) from Pierce Biotechnology, Rockford, IL, USA as per manufacturer's protocol.

Cell migration assay or wound healing assay

A549 and HOP62 cells were plated on 6-well plates in triplicates and after 24 hrs of siRNA transfections, wound were made using the pipette tip following replacement with fresh media. Cells were examined successively after 24 hrs and 48 hrs of wound formation and photographed.

Boyden chamber cell migration and cell invasion assay

BD BioCoatTM Matrigel Invasion Chambers (#354480), with 8.0 µm PET Membrane 24-well Cell Culture Inserts packaged ready-to-use in BD Falcon™ Companion Plates (#40480) and Growth Factor Reduced BD Matrigel™ Matrix, (#354230) (BD Biosciences, San Jose, CA, USA) were used in Matrigel invasion assay. Boyden chamber cell migration and cell invasion assay was performed as described previously [4]. Briefly, transwells were coated with Matrigel and then kept in an incubator at 37 °C for 1hr. After 24 hrs of transfections of A549 cells either with non-targeting siRNA (si_NT) or with siRNAs targeting UBQLN1 (si_U1), siRNA targeting UBQLN2 (si_U2-5) or combined siRNAs targeting UBQLN1 and UBQLN2 (si_U1+ si_U2-5) cells were trypsinized, washed once with PBS, resuspended in serum-free medium, and then seeded in Transwells (25,000 cells per Transwell). In the lower chamber of Transwells 10% fetal bovine serum medium was added and cells were allowed to grow on Transwells. Following total 72hrs of transfections, cells that were migrated or invaded through the matrigel to the reverse side of the inserts were rinsed with PBS, fixed in 4% formaldehyde for 30 min at room temperature, and stained with Hema 3 stain (#122-911) (Thermo Fisher Scientific Inc. Kalamazoo, MI, USA). The cells were then mounted and photographed. Total number of cells migrated or invaded through matrigel were counted and relative number of cells following loss of UBQLN1 (si_U1), UBQLN2 (si_U2-5) and combined loss of UBQLN1 and UBQLN2 (si_U1+ si_U2-5) were calculated.

Immunoprecipitation assay

293T cells were transfected either with empty vector (EV) or with FLAG-UBQLN1 (PCS2-PLIC1) and FLAG-UBQLN1 (PCS2-PLIC1-CL) for cross linking. 48 hours post transfection, cells were harvested using a cell scraper in ice-cold 1X PBS. Cells were centrifuged at 3000 rpm for 3 minutes at 4°C and PBS was aspirated out. DSP (dithiobis (succinimidyl propionate)) or Lomant's reagent (ThermoScientific 22585) was used as the cross-linking agent. Following crosslinking, cells were lysed in 0.1% CHAPS lysis buffer with protease and phosphatase inhibitors. For co-immunoprecipitation, 250ul of FLAG-M2 Affinity Gel Matrix (Sigma A2220) were washed with ice cold 1X PBS four times, followed by one wash in 0.1% CHAPS lysis buffer. Samples were then heated either at 65°C or 95°C, followed by western blot analysis with the indicated antibody. Where indicated immunoprecipitation with anti-FLAG conjugated agarose beads was performed to determine UBQLN1 interacting complexes.

Results

Loss of UBQLN1 or UBQLN2 increases cell viability, clonogenic potential and cell migration in lung adenocarcinoma cells

Previous work from our lab reported that, loss UBQLN1 or UBQLN2 induce epithelial mesenchymal transition (EMT) in lung adenocarcinoma cells [4]. During EMT, epithelial cells lose their polarity, cell to cell contacts and gain migratory and invasive properties [6,7]. In the present study, we examined siRNA-mediated knockdown of UBQLN1 and/or UBQLN2 in cell viability, clonogenic potential and cell migration of lung adenocarcinoma cells. Interestingly, we observed that loss of either UBQLN1 or UBQLN2 increases cell viability and clonogenic potential in lung adenocarcinoma cells (Fig. 1A–C). Next, we were interested to see whether combined loss of UBQLN1 and UBQLN2 exhibits additive effect on cell viability, clonogenic potential or cell migration in A549 cells. As expected, we observed

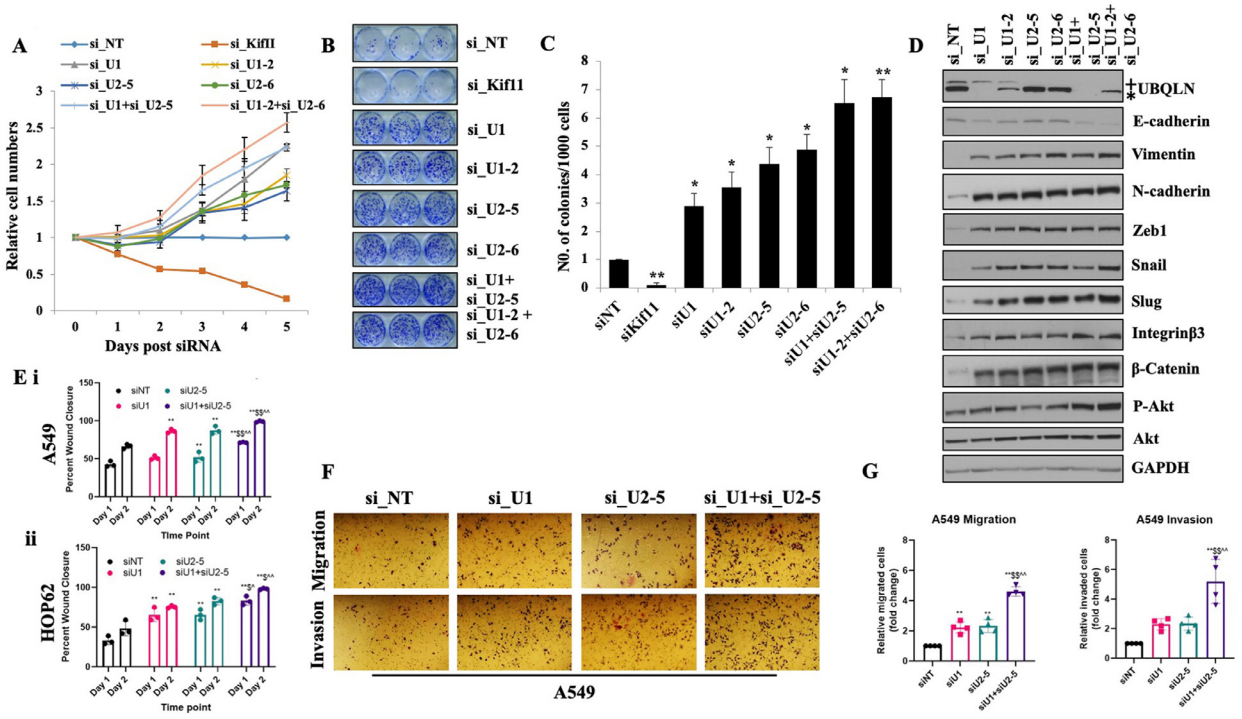

Fig. 1. Loss of UBQLN1 and UBQLN2 increases cell viability, clonogenic potential and combined loss of UBQLN1 and UBQLN2 exhibits additive effect on cell viability, clonogenic potential and induces EMT in A549 cells. Loss of UBQLN1 and UBQLN2 increases cell migration in A549 and HOP62 cells and combined loss of UBQLN1 and UBQLN2 exhibits additive effect on cell migration and cell invasion in A549 cells. (A) Cell viability assay in A549 cells. Cells (500,000) were seeded on 60mm plate and were transfected with either non targeting (si_NT) siRNA or positive control Kif11 (si_Kif11), two different siRNAs targeting UBQLN1 (si_U1 and si_U1-2), two different siRNAs targeting UBQLN2 (si_U2-5 and si_U2-6) and also combining two different siRNAs of UBQLN1 and UBQLN2 (si_U1+si_U2-5, si_U1-2+si_U2-6). After 24 hrs of transfection, cells were trypsinized and 1000 cells were reseeded in 96 well plates and cell viability was assessed for consecutive 4 days. Relative number of cells were compared by performing students' *t*-test. * = significance compared to NT (*$P < 0.05$; **$P < 0.005$). (B) Clonogenic assay in A549 cells. Cells were prepared as described in A. After 24 hrs of transfection, cells were trypsinized and 1000 cells were reseeded on 6 well plates in triplicates. Following the 10 days, cells were fixed and stained. (C) Quantification of relative number of colonies formed per 1000 number of cells seeded in B. Number of colonies formed were compared by performing students' t-test. * = significance compared to NT (*$P < 0.05$; **$P < 0.005$). (D) Western blot analysis of proteins involved in EMT. Cells were prepared as described in A. After 72 hrs of transfection, cells were harvested and analyzed for protein involved in EMT. * - UBQLN1; + - UBQLN2. (E) Cell migration assay/scratch assay in A549 and HOP62 cells. Representative bar graph showing percentage wound closure following loss of either UBQLN1, UBQLN2 or combined loss of UBQLN1 and UBQLN2. Cells were prepared as described in A. 24 hrs post siRNA transfections a pipette tip was used to scratch the dish to make a "wound". Cells were examined after wound has been formed and successively for 24hr and 48hr post wound formation, photographed and quantified. Wound closure was analyzed using a Two-way ANOVA followed by a Tukey post-hoc test. * = significance compared to NT, $ = significance compared to U1, ^ = significance compared to U2. One symbol denotes a *p*-value < 0.05, two symbols denote a *p*-value < 0.005. (F) Boyden chamber cell migration and invasion assay in A549 cells. Cells were prepared as described in A and 24 h after siRNA transfection cells were seeded into Boyden chambers without or with matrigel. The lower chamber contained media with serum, whereas the upper chamber containing the cells was without serum. 48 h later cells on the underside of the membrane were fixed and stained. (G) Quantification of relative number of cells migrated or invaded through matrigel. Migration and invasion was analyzed using a one way ANOVA followed by a Tukey post-hoc test. * = significance compared to NT, $ = significance compared to U1, ^ = significance compared to U2. One symbol denotes a *p*-value < 0.05, two symbols denote a *p*-value < 0.005.

further increase in cell viability, clonogenic potential with combined loss of UBQLN1 and UBQLN2 compared to UBQLN1 or UBQLN2 alone (Fig. 1A–C). Consistent with these findings, we also observed further decrease in expression of epithelial markers including E-cadherin and increase in expression of mesenchymal markers including N-cadherin, Zeb1, Snail and Slug and activation of β-catenin in A549 cells. Interestingly, we also observed further increase in phosphorylation of Akt following combined loss of UBQLN1 and UBQLN2 compared to UBQLN1 or UBQLN2 alone (Fig. 1D). These results provide evidence that both UBQLN1 and UBQLN2 exhibit some redundant functions in blocking tumorigenic processes in lung adenocarcinoma cells. In the present study, we observed loss of either UBQLN1 or UBQLN2 increases cell viability, clonogenic potential and we also observed further increase in cell viability, clonogenic potential and EMT markers following combined loss of UBQLN1 and UBQLN2 (Fig. 1A–D). Next, we were interested to see the role of UBQLN1 and UBQLN2 in cell migration and invasion. We performed scratch migration/wound healing assays after silencing UBQLN1 and/or UBQLN2 in A549 cells. A549 cells were transfected with either non-targeting siRNA (si_NT) or siRNAs targeting UBQLN1 (si_U1) or siRNAs targeting UBQLN2 (si_U2-5) and combined siRNA targeting UBQLN1 (si_U1) and UBQLN2 (si_U2-5). 24hrs post transfection, scratch was made using pipette tip and cells were observed for migration for consecutive two days. Interestingly, we observed that siRNA mediated knockdown of UBQLN1 or UBQLN2 increases cell migration compared to cells transfected with control siRNA (Fig. 1Ei).

A

No. of Experiments Performed	Immunoprecipitation/Mass Spectrometry Unique Peptide Count identified each experiment	
	UBQLN1	UBQLN2
1	26	7
2	9	2
3	3	5
4	32	2

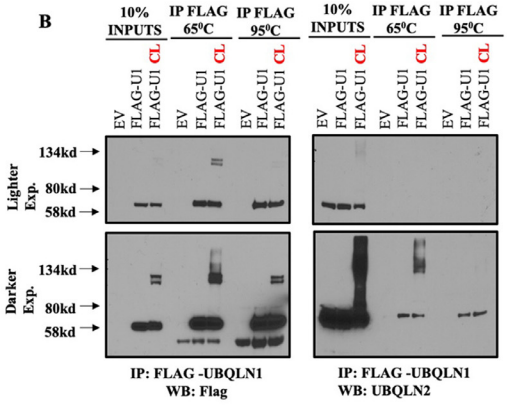

Fig. 2. UBQLN1 and UBQLN2 interacts with each other. (A) Representative chart showing number of unique peptides identified each time following IP MS/MS. 293T cells were transfected with FLAG-UBQLN1 (PCS2-PLIC1). Immunoprecipitation was performed by using flag conjugated beads to pull down UBQLN1 and endogenous UBQLN2 followed by mass spectrometry analysis. Experiment was performed four separate times and each time unique peptides were identified following IP MS/MS were represented in chart. (B) Western blot analysis of UBQLN1 interaction with UBQLN2. 293T cells were transfected either with empty vector (EV) or with FLAG-UBQLN1 (PCS2-PLIC1) and FLAG-UBQLN1 (PCS2-PLIC1-CL) following crosslinking with formalin by heating protein lysates in SDS at indicated temperatures. 72 h post transfection cells were lysed, and western blots were performed with the indicated antibody. Where indicated immunoprecipitation with anti-FLAG conjugated agarose beads was performed to determine UBQLN1 interacting complexes.

This observation was confirmed in an additional lung cancer cell line, HOP62 (Fig. 1Eii). Combined loss of UBQLN1 and UBQLN2 further increased migration of both cell lines (p-value < 0.005). Increase in cell migration following loss of UBQLN1 or UBQLN2 was further confirmed by performing boyden chamber cell migration and invasion assay (Fig. 1F). Consistent with cell migration, we also observed increase in cell invasion in A549 cells following loss of either UBQLN1 or UBQLN2 (Fig. 1G). Similar to cell migration, we observed further increase in cell invasion following combined loss of UBQLN1 and UBQLN2 (p-value < 0.005). These results provide clear evidence that, UBQLN1 and UBQLN2 plays important role in blocking cell proliferation, clonogenic potential and cell migration of lung adenocarcinoma cells.

UBQLN1 and UBQLN2 interact with each other and potentially with different client proteins

UBQLN family proteins are known to play important role in protein trafficking and proteostasis in cells, especially in cells of neuronal origin [8,9]. We and others have demonstrated that UBQLN1 and UBQLN2 are capable of forming hetero- and homo- multimers [10,11]. However, the extent to which hetero- and homo-multimers interact with substrate proteins within cells has been difficult to assess. If hetero-multimers of UBQLN1 and UBQLN2 interact with different substrates than either homo-multimer, this could be a potential mechanism by which loss of both UBQLN1 and UBQLN2 have a more dramatic phenotype than loss of either individual gene. We previously performed a number of immunoprecipitations followed by mass spectrometry identification of UBQLN1 interacting proteins [12]. In every experiment, using FLAG-UBQLN1 as bait, we identified multiple unique peptides corresponding to UBQLN2, indicating hetero-multimer formation (Fig. 2A). Dozens, if not hundreds, of additional proteins were also identified, thus it is not possible to know what combination of UBQLN1/UBQLN2/substrate are in a single complex or many different complexes. It is possible that multimers break apart following interaction with substrate or homo-multimers interact differently with substrates than hetero-multimers. To gain initial insight into these possibilities we transfected cells with FLAG-UBQLN1 and either left cells untreated or treated cells with crosslinking reagent. Cell lysates were prepared and either boiled or not and then FLAG immunoprecipitations were performed. Western blots were done with FLAG, UBQLN1 or UBQLN2 specific antibodies. Interestingly, UBQLN2 containing complexes migrated much slower on the gel, suggesting that UBQLN1/UBQLN2 containing complexes may interact with a different repertoire of substrates within cells (Fig. 2B). This observation warrants further biochemical and biophysical investigation.

Examination of mRNA expression changes following loss of UBQLN1 and/or UBQLN2 in lung cancer cells

In the present study we utilized RNAseq technology to identify gene expression alterations following loss of UBQLN1 or UBQLN2 in A549 cells. We performed siRNA mediated knockdown of UBQLN1 and UBQLN2. Comparison of gene expression profiles in A549 identified 2262 overlapping genes differentially expressed following UBQLN1 or UBQLN2 knockdown (Fig. 3A). Furthermore, we identified 2723 unique gene expression changes following UBQLN1 knockdown and 1586 unique gene expression changes following UBQLN2 knockdown in A549 cells. The top 10 most up- or down-regulated genes specific to either loss of UBQLN1 or UBQLN2 are shown in Fig. 3. RT-PCR validation of a handful of genes demonstrated similar regulation following loss of UBQLN1 in another lung cancer cell line (Fig. 3F). These genes were significantly altered following loss of UBQLN1. Importantly, there was a very strong correlation between the directionality of gene regulation following loss of UBQLN1 or UBQLN2, such that when gene expression was up in UBQLN1 loss, it was also up in UBQLN2 loss and vice versa (Fig. S1). Furthermore, to identify classes of genes that were over-represented within overlapping 2262 genes following loss of UBQLN1 and UBQLN2 in A549 cells, we performed Gene set enrichment analysis (GSEA). The top data sets that were found to be enriched with the overlapping UBQLN1/UBQLN2 genes were E2F1, G2M checkpoint and Interferon gamma signaling (Fig. S2).

Role of UBQLN family proteins, especially UBQLN1 and UBQLN2 in neurological disorders has been well established [13,14]. We have been curious about cell-type specificity of UBQLN1 and UBQLN2 function. Therefore, we also performed RNAseq analysis of neuroblastoma cell line SK-N-BE(2) following knockdown of UBQLN1 or UBQLN2. Comparison of gene expression profiles in SK-N-BE(2) cells identified 416 unique overlapping genes altered following UBQLN1 or UBQLN2 knockdown. 491 genes were found to be significantly altered following specifically UBQLN1

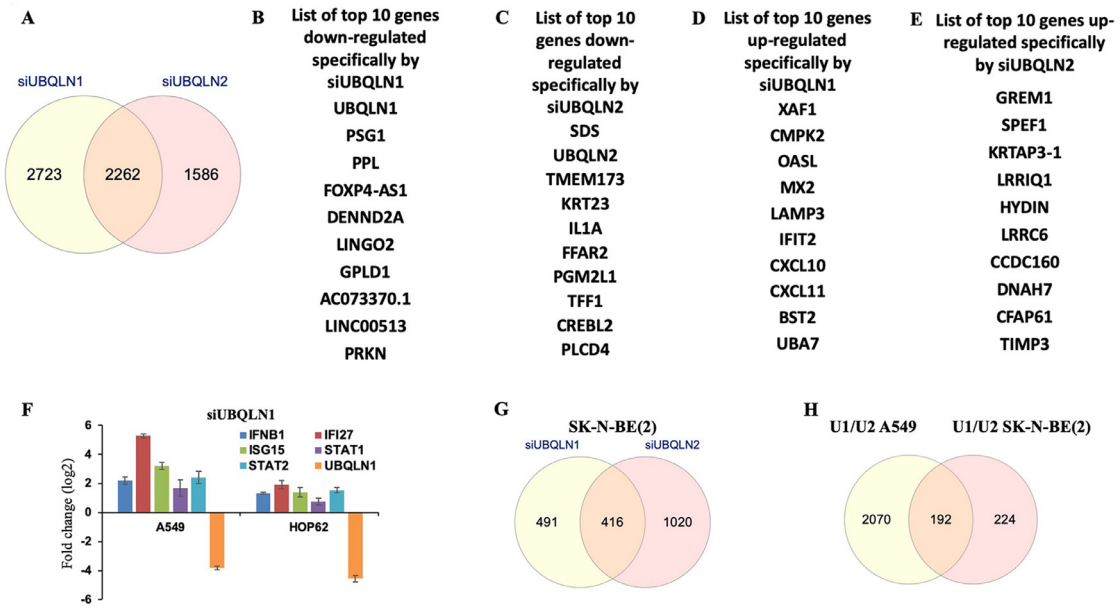

Fig. 3. RNAseq comparisons of overlapping genes differentially expressed upon UBQLN1 and UBQLN2 knockdown in A549 and SK-N-BE(2) cells. (A) Representative Venn diagram showing comparisons of overlapping genes differentially expressed upon UBQLN1 and UBQLN2 knockdown in A549 cells following RNAseq analysis. (B) Representative list of top 10 genes down-regulated specifically by siUBQLN1. (C) Representative list of top 10 genes down-regulated specifically by siUBQLN2. (D) Representative list of top 10 genes up-regulated specifically by siUBQLN1. (E) Representative list of top 10 genes up-regulated specifically by siUBQLN2. (F) Representative bar graph showing confirmation of genes that were significantly altered following loss of UBQLN1 in A549 and HOP62 cells. (G) Representative Venn diagram showing comparisons of overlapping genes differentially expressed upon UBQLN1 and UBQLN2 knockdown in SK-N-BE(2) cells following RNAseq analysis. (H) Representative Venn diagram showing comparisons of overlapping genes differentially expressed upon UBQLN1 and UBQLN2 knockdown in A549 and SK-N-BE(2) cells following RNAseq analysis.

knockdown and 1020 genes were found to be significantly altered following specifically UBQLN2 knockdown (Fig. 3G). Interestingly, when we then compared the 416 UBQLN1/UBQLN2 commonly regulated genes in SK-N-BE(2) cells with the 2262 UBQLN1/UBQLN2 commonly regulated genes in A549 cells we find 192 overlapping genes within both cell types (Fig. 3A). We further confirmed our findings regarding some common significantly altered genes following loss of UBQLN1 or UBQLN2 by performing western blot analysis (Fig. S3). We observed consistent upregulation of BRCA2, CCL2 and CXCL2 across the lung adenocarcinoma cell lines following loss of UBQLN1 and UBQLN2. It has been shown that CCL2 [15] and CXCL2 [16] overexpress in many cancers with CCL2 be linked to resistance to checkpoint inhibitor therapy [15]. Interestingly, we identified similarity in results with additional lung adenocarcinoma cell lines including HOP62 and H2009 (Fig. S3). These results clearly provide evidence that both UBQLN1 and UBQLN2 exhibits overlapping gene expression regulation.

RNAseq comparisons of overlapping genes differentially expressed upon UBQLN1 knockdown in differentiated human iPS cells and murine ES cells

There is very limited data regarding the role for UBQLN1 or UBQLN2 in normal development or in normal cell types of different origin. To begin to address this void in our understanding, we utilized human induced pluripotent stem cells (hiPSCs) and mouse embryonic stem (mES) cells, which both have the ability to differentiate into a variety of cell types, including epithelial and neuronal cells. First, we used the hiPSCs and transfected them with siRNA against UBQLN1 or non-targeting siRNA. We then differentiated cells into either neuronal or epithelial precursors and then RNAseq was performed (Fig. 4A). Data were compared between UBQLN1 deficient non-differentiated hiPSCs, neuronal precursors and epithelial precursors. Similar to previous data (Fig. 3), there was not a major overlap in gene expression changes between cell types of different origin. We did, however, identify 17 genes that were significantly altered following loss of UBQLN1 in the three cell types (Fig. 4A). Within these 17 genes were 2 genes that were also significantly changed in A549 cells following loss of UBQLN1 or UBQLN2, COL1A1 and SDC1 (Fig. 4B). Next, in order to examine if there are species specific functional similarities within different cell types, we performed RNAseq analysis following knockdown of UBQLN1 in mouse embryonic stem cells (mESCs). The mESC we used harbor doxycycline inducible shRNA against UBQLN1, and cells were differentiated into either neuronal precursors or epithelial precursors (Fig. S4). Data analyzed found that 21 overlapping genes were found to be significantly altered following shRNA mediated knockdown of UBQLN1 in unmanipulated mESC, differentiated neuronal mESC and epithelial mESC (Fig. 4C). Next, we utilized the same mES cells expressing the inducible shRNA against UBQLN1 and performed single cell RNA sequencing to determine if loss of UBQLN1 alters differentiation of cells. shUBQLN1 was induced in mES cells and then cells were differentiated to mature neuronal cells or epithelial cells (Fig. 5A). We confirmed shUbqln1 mES cells differentiation into Neuronal or Epithelial-like cells by RT-PCR analysis (Fig. S5). At the end of the differentiation protocol (Fig. 5B), cells were harvested and subjected to single cell RNA sequencing. t-Distributed Stochastic Neighbor Embedding (t-SNE) analysis was performed on the data to identify similarity and differences within the cell population (Fig. 5C). Interestingly we observed that knockdown of UBQLN1 almost completely changed the identity of cells differentiated to epithelial lineage. Conversely, loss of UBQLN1 in cells differentiated into neuronal cells revealed nearly identical cell populations. (Fig. 5C). It should be noted that knock-down of UBQLN1 in the neuronal cells was not as robust as knock-down in the epithelial cells, perhaps due to the ROSA26 promoter driving the expression of the tetracycline transactivator (Fig. S5B).

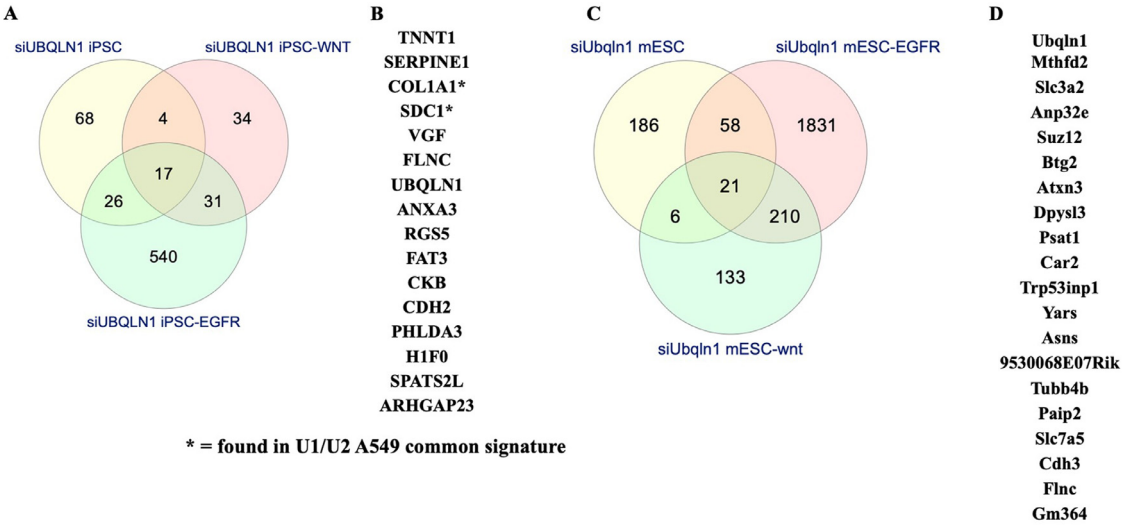

Fig. 4. RNAseq comparisons of overlapping genes differentially expressed upon UBQLN1 knockdown in differentiated iPSC-WNT and mESC-EGFR cells. (A) Representative Venn diagram showing comparisons of overlapping genes differentially expressed upon UBQLN1 knockdown in unmanipulated iPSC and differentiated iPSC-WNT epithelial and iPSC-EGF neuronal cells following RNAseq analysis. (B) Representative list of overlapping 17 genes that were significantly altered following UBQLN1 knockdown in unmanipulated iPSC, differentiated iPSC-WNT epithelial and iPSC-EGF neuronal cells following RNAseq analysis. (* = found in A549 UBQLN1/UBQLN2 knockdown common signature). (C) Representative Venn diagram showing comparisons of overlapping genes differentially expressed upon UBQLN1 knockdown in unmanipulated mESC, differentiated mESC-WNT epithelial and mESC-EGF neuronal cells following RNAseq analysis. (D) Representative list of overlapping 21 genes that were significantly altered following UBQLN1 knockdown in unmanipulated mESC, differentiated mESC-WNT epithelial and mESC-EGF neuronal cells following RNAseq analysis.

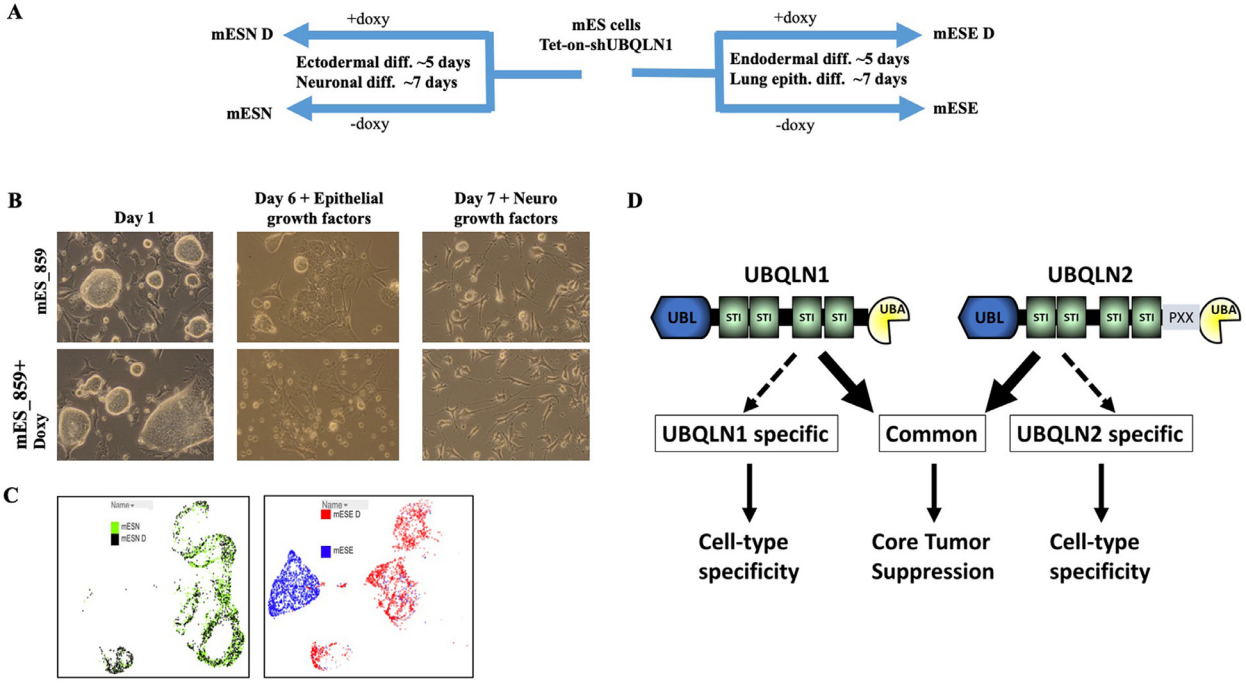

Fig. 5. shUbqln1 mES cells Differentiation into Neuronal or Epithelial-like cells. Schematic presentation of UBQLN1 and UBQLN2 having different cell type specific functions. (A) Schematic of doxycycline inducible UBQLN1 shRNA differentiation into mouse embryonic stem cell neuronal (mESN) and mouse embryonic stem cell epithelial (mESE) cells. (B) Representative microscopy images of unmanipulated mES cells and mES cells following doxycycline induction. (C) Representative t-Distributed Stochastic Neighbor Embedding (t-SNE) plots of unmanipulated neuronal/differentiated neuronal and unmanipulated epithelial/differentiated epithelial cells. Neuronal cells revealed identical transcriptional profile throughout the cell populations (green vs black spots) while loss of UBQLN1 found to alter differentiation of epithelial cells (blue vs red spots). (D) Schematic presentation of UBQLN1 and UBQLN2 having different cell type specific functions. UBQLNs has N-terminal UBL domain (ubiquitin-like), C-terminal UBA domain (ubiquitin-associated) and STI regions in the middle. Ubiquilin2 has an additional collagen-like domain between the fourth STI and UBA domains.

These data suggest that UBQLN1 and UBQLN2 have different cell type specific functions, with modest cell type independent functions.

Discussion

Ubiquilin family proteins consists of five protein members (UBQLN1-4, UBQLN-L), which are all closely related. Previous studies from other groups, reported that Ubiquilin family members have been associated with pathogenesis of numerous neurodegenerative diseases [17]. Apart from their role in neurological disorders, we showed that loss of UBQLN1 and UBQLN2 causes EMT like changes in lung adenocarcinoma cells [4]. EMT is often associated with uncontrollable increase in cell proliferation and migration [18,19]. During metastasis, tumor cells lose their polarity, cell to cell contact and migrate and colonize to secondary site [20,21]. Consistent with these findings, we observed loss of UBQLN1 and UBQLN2 increases cell proliferation and clonogenic potential in lung adenocarcinoma cells (Fig. 1A–C). Interestingly, we observed further increase in all these cellular processes following combined loss of UBQLN1 and UBQLN2 in A549 cells (Fig. 1A–D).

In an effort to find the UBQLN1 and UBQLN2 interacting protein partners, we performed IP-MS analysis. Interestingly, we identified number of unique interacting peptides with UBQLN1 and UBQLN2 (Fig. 2*A*). Previous work from our lab demonstrated a role for UBQLN1 in regulating the stability of the anti-apoptotic BCL2 family member, BCLb/BCL2L10 [12]. Further, we have identified Ubiquilin1 (UBQLN1) as a novel interaction partner of IGF1R [22]. Moreover, UBQLN has been well studied for its function in regulating cell surface receptors including Presenilins [23, 4] and GPCRs [25]. In the present study, we identified overlapping functions of UBQLN1 and UBQLN2 in regulating cell proliferation, clonogenic potential and cell migration in lung adenocarcinoma cells. Interestingly, we observed further increase in all cellular processes following loss of UBQLN1 and UBQLN2. So, we hypothesize that UBQLN1 and UBQLN2 interacts with each other and their interaction is crucial for regulating these cellular functions. We performed immunoprecipitation experiment by overexpressing UBQLN1 and immunoprecipitating endogenous UBQLN2 in 293T cells. Interestingly, following immunoprecipitation and western blot analysis we observed that UBQLN1 and UBQLN2 interacts with each other (Fig. 2B).

RNAseq is used widely for its application in the field of understanding transcriptomic dynamics [26]. In an attempt, to explore the overlapping functions and gene signatures regulated by both UBQLN1 and UBQLN2, we performed RNAseq analysis. We performed siRNA mediated knockdown of UBQLN1 and UBQLN2 in A549 cells. Interestingly, we found 2262 overlapping genes that were altered following UBQLN1 and UBQLN2 in A549 cells. 2723 genes were found to be altered by UBQLN1 knockdown and 1586 genes were found to be altered by UBQLN1 knockdown alone. We also identified top 10 genes that were significantly downregulated following loss of either UBQLN1 or UBQLN2. Interestingly most of them known to play important role in modulation of membrane structures and cytoskeletal reorganization including PPL, KRT23 and TFF1. Recently, expression of PPL has been shown to be associated with breast cancer risk in Tunisian population [27] and TFF1 has been shown to promotes EMT-like changes through an auto-induction mechanism [28]. We also identified top 10 genes that were significantly upregulated specifically by UBQLN1 or UBQLN2 including CMPK2, LAMP3 and LRRIQ1 in A549 cells. We performed gene set enrichment analysis (GSEA) of representative gene sets from overlapping 2262 genes following loss of UBQLN1 and UBQLN2 in A549 cells. Interestingly, we identified gene sets enriched in genes that are significantly associated with a phenotype including E2 factor (E2F) family of transcription factors, G2/M DNA damage checkpoint and genes involved in interferon (IFN)-mediated innate immune response (Fig. S2).

We observed overlapping important functional enriched genes sets following loss of UBQLN1 or UBQLN2. Next, we were interested whether this is cell type specific. To answer this question, we use neuroblastoma SK-N-BE(2) cells. We performed RNAseq analysis following loss of UBQLN1 and UBQLN2. Interestingly, comparison of gene expression profiles in SK-N-BE(2) cells transfected with either siRNA targeting UBQLN1 (si_U1) or siRNA targeting UBQLN2 (siU2-5) identified a set of 416 unique overlapping genes differentially expressed upon UBQLN1 and UBQLN2 knockdown (Fig. 3G). 491 and 1020 genes were found to be differentially expressed following specifically UBQLN1 and UBQLN2 knockdown. Interestingly, when we compared gene expression profiles of A549 and SK-N-BE(2) cells we observed unique 192 overlapping genes that were differentially expressed following loss of UBQLN1 and UBQLN2. This data further provides evidence of functional similarities of UBQLN1 and UBQLN2 in different cell types.

Next, we performed comparisons of overlapping genes differentially expressed upon UBQLN1 knockdown in unmanipulated iPSC and differentiated iPSC-WNT epithelial and iPSC-EGF neuronal cells following RNAseq analysis. Interestingly, we found 17 genes were significantly altered following loss of UBQLN1 in unmanipulated iPSC and differentiated iPSC-WNT epithelial and iPSC-EGF neuronal cells. Among the top 17 genes, we identified COL1A1 and SDC1 genes were most significantly altered in A549 and iPSCs following loss of UBQLN1 or UBQLN2. Collagen type I α 1 (COL1A1) is a major component of collagen type I and has been reported to be overexpressed in a variety of tumor tissues and cells. Recently, COL1A1 has been shown to promote metastasis in colorectal cancer by regulating the WNT/PCP pathway [29]. Syndecan 1 is a protein which in humans is encoded by the SDC1 gene. SDC1 involves in intracellular and extracellular matrix adhesion and regulates the activation of growth factor receptors. Recently, it has been shown that SDC1 knockdown induces epithelial–mesenchymal transition and invasion of gallbladder cancer cells via the ERK/Snail pathway [30]. Moreover, Syndecan-1 induction in lung microenvironment has been reported to support the establishment of breast tumor metastases [31]. We also performed comparisons of overlapping genes differentially expressed upon UBQLN1 knockdown in unmanipulated mESC, differentiated mESC-WNT epithelial and mESC-EGF neuronal cells following RNAseq analysis. Interestingly, we found 21 genes were significantly altered following loss of UBQLN1 in unmanipulated mESC, differentiated mESC-WNT epithelial and mESC-EGF neuronal cells. This data clearly demonstrates the functional similarities of UBQLN1 between neuronal and lung adenocarcinoma cells. We further confirmed our results, by using doxycycline inducible shUBQLN1 mESCs. We performed doxycycline inducible shUBQLN1 mESCs reprogramming into either epithelial or neuronal cells followed by RNAseq analysis. Neuronal cells revealed identical transcriptional profile throughout the cell populations while loss of UBQLN1 found to alter differentiation of epithelial cells.

Conclusions

In conclusion, in the present study we provide evidence that UBQLN1 and UBQLN2 share common cellular functions including cell proliferation, clonogenic potential and cell migration in driving EMT in lung adenocarcinoma cells. Interestingly, loss of both UBQLN1 and UBQLN2 further potentiate their tumor suppressive functions (Fig. 5D). Future work will explore in-depth analysis of signaling pathways contributed by UBQLN1 and UBQLN2 in lung cancer progression and metastasis with the hope of blocking these pathways can potentially halt the metastasis.

Declaration of Competing Interest

The authors declare that they have no known competing financial interests or personal relationships that could have appeared to influence the work reported in this paper.

CRediT authorship contribution statement

Parag P. Shah: Conceptualization, Formal analysis, Data curation, Investigation, Writing – original draft. **Kumar Saurabh:** Formal analysis, Investigation. **Zimple Kurlawala:** Investigation. **Alexis A. Vega:** Investigation. **Leah J. Siskind:** Resources, Investigation, Conceptualization, Writing – review & editing, Supervision. **Levi J. Beverly:** Resources, Investigation, Conceptualization, Writing – review & editing, Visualization, Supervision, Funding acquisition.

Acknowledgments

We thank Lavona Casson and current members of the ToTOL (Tumorigenesis and Therapeutic Outcomes Laboratory) lab, for technical assistance and Shelia Thomas and Dr. Mohammad T. Malik for valuable comments, discussion and technical advice. The work was supported by an NCI RO1 R01CA193220 to JLB, James Graham Brown Cancer Center, University of Louisville and Kosair Pediatric Cancer Program, NIH/NIGMS P20GM103436.

Supplementary materials

Supplementary material associated with this article can be found, in the online version, at doi:10.1016/j.neo.2021.11.010.

References

[1] El Ayadi A, Stieren ES, Barral JM, Boehning D. Ubiquilin-1 regulates amyloid precursor protein maturation and degradation by stimulating K63-linked polyubiquitination of lysine 688. *Proc Natl Acad Sci U S A* 2012;**109**:13416–21.

[2] Deng HX, Chen W, Hong ST, Boycott KM, Gorrie GH, Siddique N, Yang Y, Fecto F, Shi Y, Zhai H, et al. Mutations in UBQLN2 cause dominant X-linked juvenile and adult-onset ALS and ALS/dementia. *Nature* 2011;**477**:211–15.

[3] Fahed AC, McDonough B, Gouvion CM, Newell KL, Dure LS, Bebin M, Bick AG, Seidman JG, Harter DH, Seidman CE. UBQLN2 mutation causing heterogeneous X-linked dominant neurodegeneration. *Ann Neurol* 2014;**75**:793–8.

[4] Shah PP, Lockwood WW, Saurabh K, Kurlawala Z, Shannon SP, Waigel S, Zacharias W, Beverly LJ. Ubiquilin1 represses migration and epithelial-to-mesenchymal transition of human non-small cell lung cancer cells. *Oncogene* 2015;**34**:1709–17.

[5] Zhang X, Su Y, Lin H, Yao X. The impacts of ubiquilin 1 (UBQLN1) knockdown on cells viability, proliferation, and apoptosis are mediated by p53 in A549 lung cancer cells. *J Thorac Dis* 2020;**12**:5887–95.

[6] Heerboth S, Housman G, Leary M, Longacre M, Byler S, Lapinska K, Willbanks A, Sarkar S. EMT and tumor metastasis. *Clin Transl Med* 2015;**4**:6.

[7] Derynck R, Weinberg RA. EMT and cancer: more than meets the eye. *Dev Cell* 2019;**49**:313–16.

[8] Osaka M, Ito D, Suzuki N. Disturbance of proteasomal and autophagic protein degradation pathways by amyotrophic lateral sclerosis-linked mutations in ubiquilin 2. *Biochem Biophys Res Commun* 2016;**472**:324–31.

[9] Lin G, Mao D, Bellen HJ. Amyotrophic lateral sclerosis pathogenesis converges on defects in protein homeostasis associated with TDP-43 mislocalization and proteasome-mediated degradation overload. *Curr Top Dev Biol* 2017;**121**:111–71.

[10] Kurlawala Z, Shah PP, Shah C, Beverly LJ. The STI and UBA domains of UBQLN1 are critical determinants of substrate interaction and proteostasis. *J Cell Biochem* 2017;**118**:2261–70.

[11] Hjerpe R, Bett JS, Keuss MJ, Solovyova A, McWilliams TG, Johnson C, Sahu I, Varghese J, Wood N, Wightman M, et al. UBQLN2 mediates autophagy-independent protein aggregate clearance by the proteasome. *Cell* 2016;**166**:935–49.

[12] Beverly LJ, Lockwood WW, Shah PP, Erdjument-Bromage H, Varmus H. Ubiquitination, localization, and stability of an anti-apoptotic BCL2-like protein, BCL2L10/BCLb, are regulated by Ubiquilin1. *Proc Natl Acad Sci U S A* 2012;**109**:E119–26.

[13] Adegoke OO, Qiao F, Liu Y, Longley K, Feng S, Wang H. Overexpression of Ubiquilin-1 alleviates alzheimer's disease-caused cognitive and motor deficits and reduces amyloid-beta accumulation in mice. *J Alzheimers Dis* 2017;**59**:575–90.

[14] Nguyen DKH, Thombre R, Wang J. Autophagy as a common pathway in amyotrophic lateral sclerosis. *Neurosci Lett* 2019;**697**:34–48.

[15] Tu MM, Abdel-Hafiz HA, Jones RT, Jean A, Hoff KJ, Duex JE, Chauca-Diaz A, Costello JC, Dancik GM, Tamburini BAJ, et al. Inhibition of the CCL2 receptor, CCR2, enhances tumor response to immune checkpoint therapy. *Commun Biol* 2020;**3**:720.

[16] Zhang F, Jiang J, Xu B, Xu Y, Wu C. Over-expression of CXCL2 is associated with poor prognosis in patients with ovarian cancer. *Medicine* 2021;**100**:e24125 (Baltimore)-e24125.

[17] Marín I. The ubiquilin gene family: evolutionary patterns and functional insights. *BMC Evolut Biol* 2014;**14**:63.

[18] De Craene B, Berx G. Regulatory networks defining EMT during cancer initiation and progression. *Nat Rev Cancer* 2013;**13**:97–110.

[19] Pastushenko I, Blanpain C. EMT Transition states during tumor progression and metastasis. *Trends Cell Biol* 2019;**29**:212–26.

[20] Bravo-Cordero JJ, Hodgson L, Condeelis J. Directed cell invasion and migration during metastasis. *Curr Opin Cell Biol* 2012;**24**:277–83.

[21] Shenoy AK, Lu J. Cancer cells remodel themselves and vasculature to overcome the endothelial barrier. *Cancer Lett* 2016;**380**:534–44.

[22] Kurlawala Z, Dunaway R, Shah PP, Gosney JA, Siskind LJ, Ceresa BP, Beverly LJ. Regulation of insulin-like growth factor receptors by Ubiquilin1. *Biochem J* 2017;**474**:4105–18.

[23] Mah AL, Perry G, Smith MA, Monteiro MJ. Identification of ubiquilin, a novel presenilin interactor that increases presenilin protein accumulation. *J Cell Biol* 2000;**151**:847–62.

[24] Massey LK, Mah AL, Ford DL, Miller J, Liang J, Doong H, Monteiro MJ. Overexpression of ubiquilin decreases ubiquitination and degradation of presenilin proteins. *J Alzheimers Dis* 2004;**6**:79–92.

[25] N'Diaye EN, Hanyaloglu AC, Kajihara KK, Puthenveedu MA, Wu P, von Zastrow M, Brown EJ. The ubiquitin-like protein PLIC-2 is a negative regulator of G protein-coupled receptor endocytosis. *Mol Biol Cell* 2008;**19**:1252–60.

[26] Han Y, Gao S, Muegge K, Zhang W, Zhou B. Advanced applications of RNA sequencing and challenges. *Bioinform Biol Insights* 2015;**9**:29–46.

[27] Hamdi Y, Boujemaa M, Ben Rekaya M, Ben Hamda C, Mighri N, El Benna H, Mejri N, Labidi S, Daoud N, Naouali C, et al. Family specific genetic predisposition to breast cancer: results from Tunisian whole exome sequenced breast cancer cases. *J Transl Med* 2018;**16**:158.

[28] Romano E, Vllahu M, Bizzarro V, Belvedere R, Esposito R, Petrella A, Tosco A. TFF1 promotes EMT-like changes through an auto-induction mechanism. *Int J Mol Sci* 2018;**19**.

[29] Zhang Z, Wang Y, Zhang J, Zhong J, Yang R. COL1A1 promotes metastasis in colorectal cancer by regulating the WNT/PCP pathway. *Mol Med Rep* 2018;**17**:5037–42.

[30] Liu Z, Jin H, Yang S, Cao H, Zhang Z, Wen B, Zhou S. SDC1 knockdown induces epithelial-mesenchymal transition and invasion of gallbladder cancer cells via the ERK/Snail pathway. *J Int Med Res* 2020;**48** 300060520947883.

[31] Chute C, Yang X, Meyer K, Yang N, O'Neil K, Kasza I, Eliceiri K, Alexander C, Friedl A. Syndecan-1 induction in lung microenvironment supports the establishment of breast tumor metastases. *Breast Cancer Res* 2018;**20**:66.